Lattice dynamics of α uranium

J. Bouchet
CEA-DAM, DPTA, Bruyères-le-Châtel, France
(Received 2 January 2008; published 29 January 2008)

The lattice dynamics of α uranium have been known for almost 30 years but until now no theory has been able to successfully reproduce these experimental data. In this paper, we present the *ab initio* phonon spectrum of α-U. We compare the 0 K calculated spectrum with the neutron-scattering data obtained at room temperature and pay particular attention to its anomalies. We then predict the behavior of lattice dynamics of uranium as a function of pressure. Using interatomic force constants derived from our calculations, we confirm that a charge density wave state is formed at low temperature in a uranium metal.

DOI: 10.1103/PhysRevB.77.024113 PACS number(s): 71.45.Lr, 63.20.D−, 71.20.Gj

I. INTRODUCTION

Uranium is one of the most intriguing materials with many puzzling properties. Its ground state structure, α-U, is unique among pure metals because of its orthorhombic symmetry. For the moment, it is also the only element in the Periodic Table where we observe a charge density wave (CDW) state. To elucidate the nature of these features at low temperatures, several decades of experimental works were necessary. This lead to the discovery of the anomalies in the behavior of the uranium elastic constants by Fisher and McSkimin[1] and of the CDW state by Smith *et al.*[2] At this point, it became clear that the 43 K phase transition was related with the formation of an incommensurately modulated structure, due to a CDW. It took another decade to fully characterize the CDW and the three components, q_x, q_y, q_z, of the lattice distortion vector $\mathbf{q}$. We now know that the second phase transition observed at 37 K is associated with the lock-in of the q_x component and the transition at 22 K with the lock-in of the two other components. Then, below 22 K, the three components of the CDW are commensurate with the underlying lattice and the $\mathbf{q}$ vector is given by

$$\mathbf{q}(T < 22\ \mathrm{K}) = \frac{1}{2}\mathbf{a}^* + \frac{1}{6}\mathbf{b}^* + \frac{5}{27}\mathbf{c}^*, \tag{1}$$

where $\mathbf{a}^*$, $\mathbf{b}^*$, and $\mathbf{c}^*$ are the reciprocal lattice vectors. All these results are presented in the review of Lander *et al.*[3]

One of the highlight of this quest to understand the physical properties of U was the neutron inelastic scattering experiments of Crummett *et al.*[4] to determine the phonon-dispersion curves. They revealed a softening in the Σ_4 phonon branch at a wave vector of 0.5 $\mathbf{a}^*$. With a group-theory analysis, they could identify this mode with a primarily opticlike mode propagating in the [100] direction and so relate the phonon softening with the anomalies observed for the c_{11} elastic constant. Unfortunately, to reproduce their dispersion curves, they needed a six-neighbor modified shell model with no less than 27 adjustable parameters. This large number of adjustable parameters calls for a more fundamental approach and we will show how the analysis of the *ab initio* interatomic force constants (IFCs) helps us to understand the origin of the CDW phenomena in U. The decisive experiment was performed a year later when Smith *et al.*[2] followed the behavior of the Σ_4 phonon branch with temperature. The frequency of this mode near q_x=0.5 strongly decreases with temperature until it is zero, typical of a soft-mode transition. Smith *et al.*[2] concluded for a doubling of the unit cell in the x direction and a lattice distortion from the presence of a CDW.

There is a number of fundamental questions in materials science associated with the lattice dynamics of the light actinides and, in particular, of α-U. Issues concerning their melting points, the evolution of their elastic constants with temperature, or the elastic anisotropy, for example, cannot be solved without knowing their phonon-dispersion curves. For the moment, CDW has only been observed in U at low temperatures and pressures but we can speculate for other elements of this series. Unfortunately, experiments or calculations for the light actinides are far from being straightforward. Experimentally, the difficulty comes from obtaining and manipulating single crystals. Theoretically, the calculations are significant and the f electron behavior can be difficult to describe with standard approximations as the local density or generalized gradient approximations. However recently, a lot of works has emerged to bring new results on this matter. Using inelastic x-ray scattering, experiments have been successfully performed on U (Refs. 5 and 6) and Pu.[7,8] To our knowledge, there is only one fully *ab initio* spectrum for an f element, namely, Th.[9] However, with only one f electron and a fcc structure, Th does not show all the complexity found in the other light actinides, and so the conclusions obtained for this element may not pertain for the other actinides. The spectrum of fcc plutonium was obtained by Dai *et al.*[10] using dynamical mean field theory. This work brought ideas and insight into lattice dynamical properties of Pu and more generally into the f electron behavior. However, the difficulty to treat the strongly correlated f electrons of fcc Pu and the approximations made to handle this problem limited the conclusions of these results. We can also mention the work done on $PuCoGa_5$ by Raymond *et al.*[11] using the LDA+U technique.

This paper is organized as follows. First, we will present the computational details of our calculations. In the second part, we will show the phonon spectrum obtained using density functional perturbation theory (DFPT) for uranium metal at equilibrium volume. Then, we will discuss the effect of the pressure on the lattice dynamics of uranium. Finally, before the conclusions, we will analyze the interatomic force constants to shed light on the CDW state.

TABLE I. Experimental (Ref. 22) (Expt.) and theoretical equilibrium volume V (Å^3) and bulk modulus B (GPa) for U. FP stands for the all-electron method (FPLMTO) (Ref. 19) and PP is our results.

	b/a	c/a	y	V	B
PP	2.04	1.75	0.10	20.2	138
FP	2.05	1.75	0.10	20.4	136
Expt.	2.05	1.74	0.10	20.8	104

II. COMPUTATIONAL DETAILS

Our first principles calculations are performed within the generalized gradient approximation (GGA) as parametrized by Perdew[12] and implemented in the ABINIT package.[13,14] Dynamical matrices are calculated in a $12\times12\times12$ **q**-point grid and a Fourier interpolation is used to obtain phonon frequencies in the other points of the Brillouin zone. This density of **q** point is essential to reproduce the details of the α-U phonon spectrum. Technical details on the computation of responses to atomic displacements can be found in Ref. 15, while Ref. 16 presents the subsequent computation of dynamical matrices and interatomic force constants. The norm conserving pseudopotential (PP) we used in this work[17] needed a 180 Ry cutoff to achieve a 1 mRy/at. and a 0.01 THz convergence on the energy differences and phonon frequencies, respectively. The pressure was obtained using the stress tensor, with a 0.1 GPa convergence. We have included the spin-orbit coupling in our calculations and as for Th, we found no influence on the phonon frequencies.

III. EQUILIBRIUM VOLUME

The crystal structure of α-U is well reproduced by our DFT-GGA calculations, and in agreement with previous calculations, see Table I.

We present in Fig. 1 our results for the lattice dynamics of α-U. The calculations have been performed at the theoretical equilibrium volume. This point is important since the pressure has a great influence on the phonon frequencies. We also show on this figure the experimental neutron-scattering data of Crummett *et al.*[4] obtained at room temperature. We have followed their notations to label the branches. Note that the frequencies of the branches Σ_1, Σ_4, and Λ_1 are solutions of a 2×2 submatrix in the block-diagonalized dynamical matrix.[4] Therefore, these branches do not cross and their polarization vectors are mixtures of acoustic- and opticlike motions. In the figure, the red and the blue lines represent branches which are mostly optic- and acousticlike, respectively. Following Crummett *et al.*,[4] the experimental points are represented by opened and filled symbols for modes which appears to be primarily opticlike and acousticlike, respectively.

The first thing one notices is the good agreement between experiment and theory, the most remarkable result being certainly obtained for the [100] direction where the complexity of the spectrum is clearly reproduced. The best agreement is obtained for the acoustic branches, with the exception of the dip in the Σ_1 branch which will be discussed in the next paragraph at the same time as Σ_4. Even the slight depression observed in the Σ_3 branch is confirmed by our calculations.

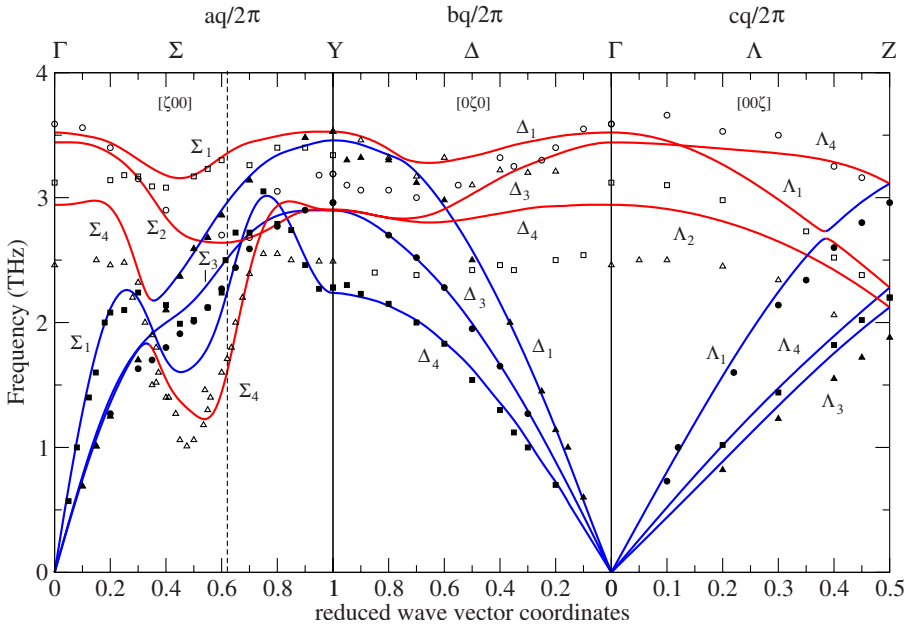

FIG. 1. (Color online) Calculated phonon-dispersion curves for α-U at the lattice parameter corresponding to static equilibrium. Blue lines represent modes which appear to be primarily acousticlike, while red lines represent modes which are mostly opticlike. Experimental neutron-scattering data (Ref. 4) are denoted by triangles.

TABLE II. Elastic constants (GPa) of α-U.

	C_{11}	C_{22}	C_{33}	C_{44}	C_{55}	C_{66}	C_{12}	C_{13}	C_{23}	B
This study	285	221	324	136	93	89	66	17	140	144
FP	300	220	320	150	93	120	50	5	110	130
Expt. (T=300 K)	215	199	267	124	73	74	47	22	108	115
Expt. (T=0 K)	210	215	297	145	95	87				

Furthermore, the slope of these branches near the Γ point seems really close to the experimental data. This can be confirmed by a comparison of the elastic constants which are related to sound velocities $d\omega/dq$ near Γ. Our results are presented in Table II and compared to experiments at T =300 K (Ref. 18) and extrapolated at T=0 K and to previous calculations.[19] We found a reasonable agreement with experimental data as expected from the phonon spectrum and our values confirm those obtained by finite-difference method.[19]

Largest discrepancies between theory and experiment are observed for the optical branches compared to the results obtained on the acoustic ones. Our most important result concerns the Σ_4 branch. The experience of Smith *et al.*[2] showed how the CDW state is related to a drastic softening of the Σ_4 phonon in temperature. In our spectrum, the dip in this branch is present but slightly above the experimental one. In their experiment, Smith *et al.* observed a large decrease of the frequency of the Σ_4 branch as the temperature is lowered. The value goes from 1.01 THz at 300 K to 0 THz around 70 K.[3] This value means of course that the structure is unstable; the unit cell is doubled in the [100] direction. This corresponds to the first CDW transition from α to α_1 structure. Then, the frequency of the Σ_4 branch rises again to recover at 10 K approximately the same value as at 100 K (around 0.8 THz). It is difficult to extrapolate a value at T=0 K from these results. From our calculations, we predict a value of 1.24 THz. However, this value is very sensible to the volume used to calculate the phonon frequencies; we will show this drastic effect when we apply pressure in the next section. The theoretical and experimental minima in the Σ_4 branch does not coincide, we predict a minimum for q=0.54 at T=0 K, while experimentally the minimum is around q=0.475 at room temperature. A displacement of the minimum of the Σ_4 branch as the temperature is lowered has been observed in the experiment of Smith *et al.*[2] but not as important as what we found here. They found a minimum for q=0.495 at 10 K. We also observe in our spectrum a large anomaly in the Σ_1 branch, much more pronounced than at room temperature. This suggests a softening of this branch in temperature similar to the softening of the Σ_4 branch. Crummett *et al.*[4] mentioned a value for the frequency of this branch at q=0.5 of 1.4 THz at 160 K compared to 2.0 THz at room temperature. At 0 K, we obtain a value of 1.73 THz. As said previously, the polarization vector of the Σ_4 mode corresponds to longitudinal opticlike motions. The motions associated with the lower Σ_1 mode are primarily longitudinal acousticlike.[4] Therefore, these two modes correspond to out-of-phase and in-phase atomic displacements in the x direction. The phase associated with the atomic motions involved in the CDW in the x direction is $(99 \pm 3)°$.[20] So, this displacement is essentially optic but also contains a small acoustic part. Then, it is not surprising to observe in the phonon spectrum the signature of the CDW in the Σ_4 but also in the Σ_1 branch.

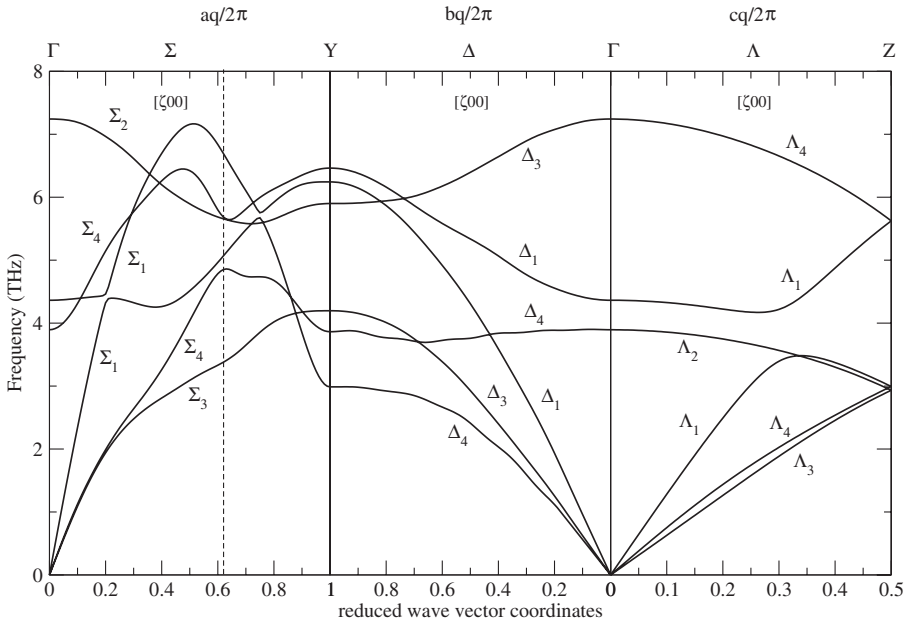

FIG. 2. Calculated phonon-dispersion curves for α-U at a volume of 15 Å^3 corresponding to a pressure of 85 GPa.

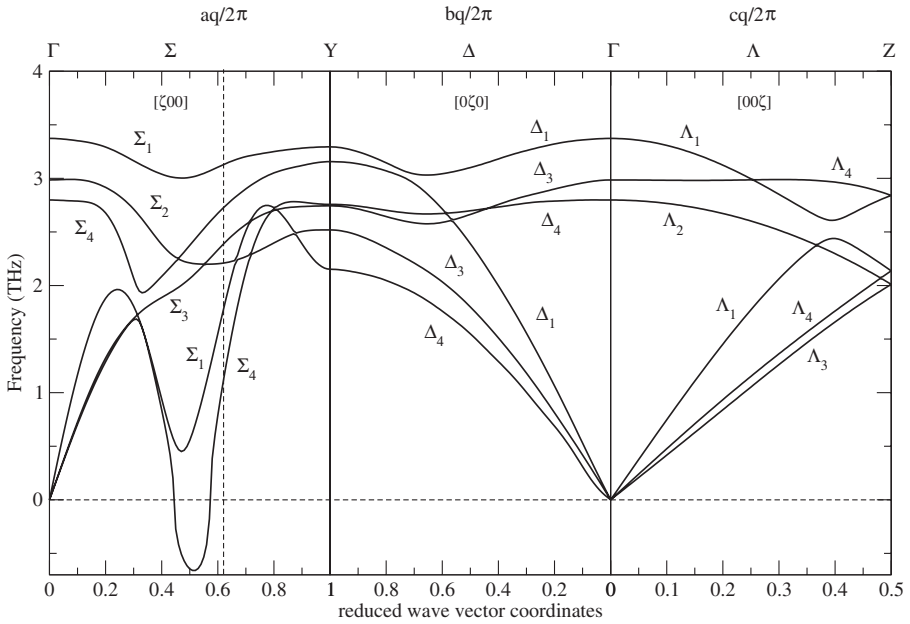

FIG. 3. Calculated phonon-dispersion curves for α-U for a volume of 21 Å^3 corresponding to a pressure of −5 GPa.

The largest discrepancies between theory and experiment are observed in the optical branches of the two other directions, [010] and [001]. First of all, in their paper, Crummett *et al.*[4] mentioned that the measurements of the Δ_1 and Δ_3 branches were the most difficult to realize due to the weakness of the phonon peak intensities. In fact, they obtained the largest uncertainties of their measurements for these two modes with an average of 0.15 THz. However, even for the other optical modes, the uncertainties are large, around 0.12 THz. This can partially explain the discrepancies. Another part comes certainly from the temperature difference between the calculations and the measurements. Our spectrum is obtained for a temperature of 0 K, so below the transition temperature toward the CDW state. Unfortunately, Smith *et al.*[2] only observed the Σ_4 mode at low temperatures, so the effect on the other modes is not known experimentally. The largest displacement in the CDW occurs in the [100] direction, almost six times larger than the other motions;[3] we have discussed its effect on the longitudinal branches Σ_1 and Σ_4. The transverse optical branches associated with atomic displacements along the [100] direction are Δ_4 and Λ_2 for the [010] and [001] directions, respectively. This could explained why we observed the largest discrepancies between theory and experiment for these two branches.

IV. EFFECT OF THE PRESSURE

Experimentally, the evolution of the Σ_4 branch in temperature is well known. However, little is known about the effect of pressure on the phonon spectrum of U. To our knowledge, there is only one experimental result for a hydrostatic pressure of 0.5 GPa.[21] This experiment shows that the Σ_4 mode shifts to higher frequency. This result is in agreement with the fact that the pressure reduces the formation of CDW which explains the softening observed in this branch. We have calculated the lattice dynamics of α-U for two volumes, below and above the equilibrium one, to study the effect of pressure on the phonon frequencies. The α-U structure has been fully relaxed at these two volumes. The results are shown in Figs. 2 and 3 corresponding to 85 and −5 GPa. To analyze in more detail the behavior of Σ_1 and Σ_4, we have reported in Fig. 4 the evolution of these two modes for several pressures, indicating also their primary character. Experimentally, α-U is stable to at least 100 GPa.[22] This result is confirmed by our calculations. There is no soft mode developing with pressure and we found no imaginary frequency at 85 GPa. On the other hand, at a volume corresponding to a small dilatation with a pressure of −5 GPa, close to the experimental volume, the frequencies in the middle of the Σ_4 branch are imaginary (plotted with negative values), with a minimum close to $q=0.5$. The α-U structure is therefore unstable toward a doubling of the unit cell. This is similar to what is found when the temperature decreased and when U undergoes the first phase transition at 43 K. In fact, at the theoretical equilibrium volume, the α-U structure is at the edge of being unstable. This result has already been found by Fast *et al.*[23] by comparing the total energies of the α-U and the α_1-U structures as a function of pressure. They have shown a phase transition from the distorted to the undistorted structure at 98% of the experimental equilibrium volume.

The Σ_1 and Σ_4 branches change drastically with pressure and show a similar behavior. Under decompression, these two branches strongly soften. Under compression, the softening rapidly disappears and the lower Σ_4 branch is more and more acousticlike. At a pressure of 10 GPa, the two dips have almost disappeared. The minimum observed around $q=0.5$ in the Σ_4 mode moves toward larger values of the q vector as the pressure increases. Experiments would be of great interest to confirm these results.

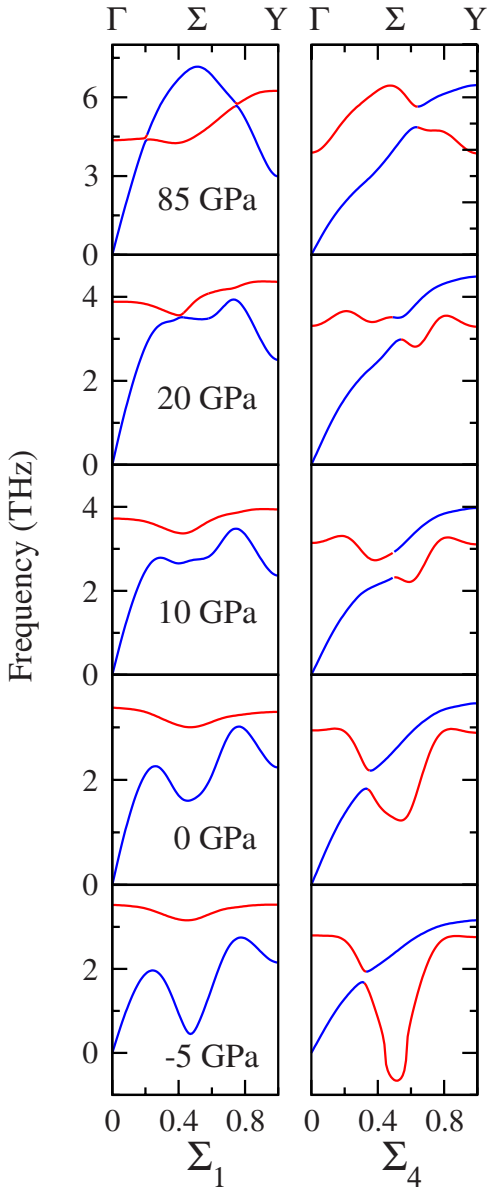

FIG. 4. (Color online) Calculated Σ_1 and Σ_4 modes of α-U at different pressures. We have indicated the primary character of the branches. Blue lines represent modes which appear to be primarily acousticlike, while red lines represent modes which are mostly opticlike.

V. INTERATOMIC FORCE CONSTANTS

Complementary and highly instructive information are obtained by the direct examination of the real-space IFCs. Due to the too large number of parameters, the two precedent attempts made to understand the relationship between forces and lattice dynamics have been unsuccessful.[4,24] The IFC's $\Phi_{\alpha\beta}(i\kappa;j\kappa')$ are defined as the second derivatives of the ground state energy of the solid with respect to the displacements of two atoms and relate the force $F_\alpha(i\kappa)$ along direction α on atom κ in cell i and the displacement $\Delta\tau_\beta(j\kappa')$ along direction β of atom κ' in cell j by the following expression:

TABLE III. Self-force constants (hartree/bohr^2).

	85 GPa	20 GPa	0 GPa	−4 GPa
x	0.2767	0.1080	0.0539	0.0403
y	0.2164	0.1249	0.0870	0.0767
z	0.2549	0.1337	0.0809	0.0659

$$F_\alpha(i\kappa) = -\Phi_{\alpha\beta}(i\kappa;j\kappa') \cdot \Delta\tau_\beta(j\kappa'). \quad (2)$$

First, we examine the self-force constant (SFC), meaning the force on a single isolated atom at a unit displacement from its crystalline position, all the other atoms remaining fixed, see Table III. The SFCs are positive for all the volumes considered here and for the three directions. In consequence, the atoms are always stable against isolated atomic displacement, only a cooperative motion of different atoms can lower the total energy and generate an instability, as observed in Fig. 4. At high pressure, the SFC in the x direction is the more important, 0.277 hartree/bohr^2 compared to 0.216 and 0.255 hartree/bohr^2 for the y and z directions, respectively. The situation is reversed at low or negative pressures. The SFC in the x direction is the smallest one, 0.040 compared to 0.077 and 0.066 hartree/bohr^2 for the y and z directions, respectively.

For other IFC tensors, we adopt the system of coordinates in which axis 1 is along the bond direction; axis 2 is the orthogonalized direction with respect to axis 1 of the force on atom κ due to the displacement of atom κ' along axis 1—in case it does not vanish—and axis 3 is perpendicular to axes 1 and 2. The longitudinal IFC (LIFC) Φ_{11} corresponding to the pressures of Fig. 4 are listed in Table IV. The full force constant tensor is given in Table V for several shells of neighbors. The IFCs are strongly directional; the longitudinal component is always the most important component of the IFC tensor. Let us focus on the second shell of nearest neighbors (NN=2) which contains the first neighbor in the [100] direction. This LIFC shows a unique behavior by changing its sign with pressure. Negative at high pressure, this LIFC becomes the only positive one at the equilibrium volume and under decompression. This means that the direction of the force induced by the displacement of the generic atom on the two nearest atoms in the [100] direction is reversed with pressure, see Fig. 5. Its absolute value is divided by almost 10 between 85 and 20 GPa when the other ones are divided by 3 at most. Moreover, this LIFC is also the only one to

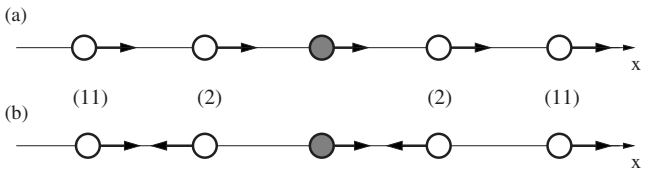

FIG. 5. Forces induced along the [100] direction by the unit displacement of a generic atom (in gray) at (a) $V=18$ Å^3 and (b) the equilibrium volume. The arrows starting from white atoms represent the direction of the forces. The numbers indicate the shell to which the neighbors belong.

TABLE IV. Longitudinal interatomic force constants Φ_{11} (hartree/bohr^2) between different pairs of atoms for α-U at four different pressures. One atom is at the origin, while the coordinates of the second atom are expressed in units of a, b, and c axes. The first column indicates the number of the shell NN to which the second atoms belong, while the number in the parentheses is the number of neighbors of the shell NN. The last column is the IFC of Pa in the α-U structure.

NN	Coordinate	85 GPa	20 GPa	0 GPa	−4 GPa	Pa II (25 GPa)
1 (2)	$(0,2y,1/2)$	−0.0945	−0.0380	−0.0157	−0.0100	−0.0255
2 (2)	(1, 0, 0)	−0.0810	−0.0096	+0.0091	+0.0129	−0.0068
3 (4)	$(1/2,1/2,0)$	−0.0453	−0.0196	−0.0110	−0.0091	−0.0262
4 (4)	$(1/2,-1/2+2y,1/2)$	−0.0371	−0.0195	−0.0132	−0.0115	−0.0221
5 (4)	$(1,2y,1/2)$	−0.0195	−0.0104	−0.0069	−0.0058	+0.0016
6 (4)	$(1/2,1/2+2y,1/2)$	−0.0062	−0.0051	−0.0038	−0.0034	−0.0023
7 (2)	(0, 0, 1)	−0.0076	−0.0073	−0.0066	−0.0063	−0.0002
8 (4)	$(3/2,1/2,0)$	−0.0048	−0.0008	+0.0005	+0.0009	−0.0007
9 (4)	$(3/2,-1/2+2y,1/2)$	+0.0001	+0.0001	0.0000	0.0000	−0.0011
10 (2)	$(0,-1+2y,1/2)$	−0.0035	−0.0020	−0.0018	−0.0015	−0.0051
11 (2)	(2, 0, 0)	−0.0020	−0.0069	−0.0083	−0.0082	−0.0077
12 (4)	(1, 0, 1)	−0.0006	0.0002	−0.0004	+0.0004	+0.0005

increase under decompression while the other LIFCs decay. At −5 GPa, when the crystal is clearly unstable, this LIFC is the dominant one, 30% larger than the LIFC between first nearest neighbors which is the strongest term for all the other pressures. We see in Table V the other components of the IFC tensor for the second shell of neighbors. The transverse components Φ_{22} and Φ_{33} decrease rapidly with pressure and become almost negligible. Φ_{12} indicates that the force induced by the displacement of the first neighbor along the x axis is not purely longitudinal but also contains a component in the y direction. As NN increases, the magnitude of LIFCs decays and becomes close to zero, with the exception of the 11th shell (about five times larger than the preceding shell, see Table IV). This shell contains the second nearest neighbor in the x direction. All the components of this IFC tensor are surprisingly stable with pressure, see Table V. Φ_{11} is only significant at low pressures, and it is negative, contrary to the LIFC with the first nearest neighbors in this direction. A motion of the central atom will therefore induce an out-of-phase motion of the first and second nearest neighbors in the x direction, see Fig. 5. This is exactly the optical displacements of the atoms observed in the CDW state. In their attempt to reproduce their neutron-scattering data, Crummett *et al.*[4] already noticed that it was essential to include the forces to 11 neighbors to reproduce the dips in the Σ_4 and Σ_1 branches.

In the actinide series, a CDW state has only been observed in U. We have investigated the α-U structure found, in pressure, in a Pa metal (Pa II),[25] which is the element next to the left of U in the actinide series. The α-U structure has been relaxed for Pa at a volume close to the phase transition with the bct structure. The last column of Table IV shows our results for Pa. The values are comparable to what is found, in pressure, in U; the IFC with the second shell of neighbors is small and negative. We have reproduced the calculations on the Pa II structure for different volumes and reach the same

TABLE V. Interatomic force constant matrix (hartree/bohr^2) in local coordinates (see text) for the first, second, and eleventh shell of neighboring atoms.

NN	20 GPa	0 GPa	−4 GPa
1	$\begin{pmatrix} -0.0380 & +0.0053 & 0.0000 \\ +0.0053 & -0.0014 & 0.0000 \\ 0.0000 & 0.0000 & -0.0034 \end{pmatrix}$	$\begin{pmatrix} -0.0157 & +0.0056 & 0.0000 \\ +0.0056 & -0.0048 & 0.0000 \\ 0.0000 & 0.0000 & -0.0037 \end{pmatrix}$	$\begin{pmatrix} -0.0100 & +0.0057 & 0.0000 \\ +0.0057 & -0.0053 & 0.0000 \\ 0.0000 & 0.0000 & -0.0035 \end{pmatrix}$
2	$\begin{pmatrix} -0.0096 & +0.0003 & 0.0000 \\ +0.0003 & +0.0039 & 0.0000 \\ 0.0000 & 0.0000 & +0.0031 \end{pmatrix}$	$\begin{pmatrix} +0.0091 & +0.0016 & 0.0000 \\ -0.0016 & +0.0005 & 0.0000 \\ 0.0000 & 0.0000 & +0.0018 \end{pmatrix}$	$\begin{pmatrix} +0.0129 & +0.0019 & 0.0000 \\ -0.0019 & -0.0002 & 0.0000 \\ 0.0000 & 0.0000 & +0.0015 \end{pmatrix}$
11	$\begin{pmatrix} -0.0069 & +0.0019 & 0.0000 \\ -0.0019 & -0.0010 & 0.0000 \\ 0.0000 & 0.0000 & -0.0021 \end{pmatrix}$	$\begin{pmatrix} -0.0083 & +0.0016 & 0.0000 \\ -0.0016 & -0.0007 & 0.0000 \\ 0.0000 & 0.0000 & -0.0019 \end{pmatrix}$	$\begin{pmatrix} -0.0082 & +0.0015 & 0.0000 \\ -0.0015 & -0.0006 & 0.0000 \\ 0.0000 & 0.0000 & -0.0018 \end{pmatrix}$

conclusions. This suggests that no CDW state can be observed in the Pa II structure. We repeat this calculation on a hypothetic α-U structure of Pu. We found the structure completely unstable, preventing any assumption about the presence or not of a CDW in this element. A study of the phonon spectrum of the α-Pu structure is certainly necessary to start answering this question.

VI. CONCLUSION

We have successfully obtained the lattice dynamics of α-U at 0 K and as a function of pressure. We have shown how the dips in the Σ_4 and Σ_1 branches are strongly reduced by pressure. This should now be confirmed by experiments. The analysis of the interatomic force constants has shown the importance of the 11th shell of neighbors and the unusual behavior of the LIFC with first neighbors in the [100] direction. After the phonon spectrum of Th, this proves that the description of the light actinide phonons can be accurately obtained by DFPT. This is of fundamental interest to understand the thermodynamics and the complex phase diagrams of this class of materials.

ACKNOWLEDGMENTS

We acknowledge useful discussions with R. C. Albers, Gilles Zerah, Stéphane Mazevet, Francois Jollet, Francois Bottin, and Bernard Amadon.

[1] E. S. Fisher and H. J. McSkimmin, Phys. Rev. **124**, 67 (1961).
[2] H. G. Smith, N. Wakabayashi, W. P. Crummett, R. M. Nicklow, G. H. Lander, and E. S. Fisher, Phys. Rev. Lett. **44**, 1612 (1980).
[3] G. H. Lander, E. S. Fisher, and S. D. Bader, Adv. Phys. **43**, 1 (1994).
[4] W. P. Crummett, H. G. Smith, R. M. Nicklow, and N. Wakabayashi, Phys. Rev. B **19**, 6028 (1979).
[5] M. E. Manley, B. Fultz, R. J. McQueeney, C. M. Brown, W. L. Hults, J. L. Smith, D. J. Thoma, R. Osborn, and J. L. Robertson, Phys. Rev. Lett. **86**, 3076 (2001).
[6] M. E. Manley, G. H. Lander, H. Sinn, A. Alatas, W. L. Hults, R. J. McQueeney, J. L. Smith, and J. Willit, Phys. Rev. B **67**, 052302 (2003).
[7] J. Wong, M. Krisch, D. L. Faber, F. Ocelli, A. J. Schwartz, T.-C. Chiang, M. Wall, C. Boro, and R. Xu, Science **301**, 1078 (2003).
[8] J. Wong, M. Wall, A. J. Schwartz, R. Xu, M. Holt, H. Hong, P. Zschack, and T.-C. Chiang, Appl. Phys. Lett. **84**, 3747 (2004).
[9] J. Bouchet, F. Jollet, and G. Zerah, Phys. Rev. B **74**, 134304 (2006).
[10] X. Dai, S. Savrasov, G. Kotliar, A. Migliori, H. Ledbetter, and E. Abrahams, Science **300**, 953 (2003).
[11] S. Raymond *et al.*, Phys. Rev. Lett. **96**, 237003 (2006).
[12] J. P. Perdew, K. Burke, and M. Ernzerhof, Phys. Rev. Lett. **77**, 3865 (1996).
[13] The ABINIT code is a common project of the Catholic University of Louvain (Belgium), Corning Incorporated, CEA (France) and other collaborators (http://www.abinit.org).
[14] X. Gonze *et al.*, Comput. Mater. Sci. **25**, 478 (2002).
[15] X. Gonze, Phys. Rev. B **55**, 10337 (1997).
[16] X. Gonze and C. Lee, Phys. Rev. B **55**, 10355 (1997).
[17] N. Richard, S. Bernard, F. Jollet, and M. Torrent, Phys. Rev. B **66**, 235112 (2002).
[18] E. S. Fisher and H. J. McSkimin, J. Appl. Phys. **29**, 1473 (1958).
[19] P. Söderlind, Phys. Rev. B **66**, 085113 (2002).
[20] J. C. Marmeggi, A. Delapalme, G. H. Lander, C. Vettier, and N. Lehner, Solid State Commun. **43**, 577 (1982).
[21] H. G. Smith and G. H. Lander, Phys. Rev. B **30**, 5407 (1984).
[22] T. Le Bihan, S. Heathman, M. Idiri, G. H. Lander, J. M. Wills, A. C. Lawson, and A. Lindbaum, Phys. Rev. B **67**, 134102 (2003).
[23] L. Fast, O. Eriksson, B. Johansson, J. M. Wills, G. Straub, H. Roeder, and L. Nordström, Phys. Rev. Lett. **81**, 2978 (1998).
[24] D. O. V. Ostenburg, Phys. Rev. **123**, 1157 (1961).
[25] R. G. Haire, S. Heathman, M. Idiri, T. Le Bihan, A. Lindbaum, and J. Rebizant, Phys. Rev. B **67**, 134101 (2003).